INSTITUTE FOR HIGH ENERGY PHYSICS


IFVE
IHEP 93-153

A.A. Lednev

# SEPARATION OF THE OVERLAPPING ELECTROMAGNETIC SHOWERS IN THE CELLULAR GAMS-TYPE CALORIMETERS

Protvino 1993

UDK 539.1.074

M–24


## Abstract

A.A. Lednev. Separation of the overlapping electromagnetic showers in the cellular GAMS-type calorimeters: IHEP Preprint 93-153. — Protvino, 1993. — p. 10, figs. 17, refs.: 3.

The structure of gamma reconstruction program for the GAMS spectrometer is described. Reconstruction efficiencies of two and three space-overlapping showers for detectors with different cell sizes are presented.

## Аннотация

А.А. Леднев. Разделение перекрывающихся электромагнитных ливней в ячеистых калориметрах типа ГАМС: Препринт ИФВЭ 93-153. — Протвино, 1993. — 10 с., 17 рис., библиогр.: 3.

Описана структура разработанной для спектрометра ГАМС программы реконструкции гамма-квантов. Приведены оценки эффективностей разделения двух и трех перекрывающихся электромагнитных ливней для детекторов с различным размером ячейки.




## 1. Cell energy deposit calculations

In the previous paper [1] an approximation of electromagnetic shower profile observed in the GAMS spectrometer [2] (without optical grease between the lead-glass radiators and photomultipliers) has been obtained:

$$\Phi(r) = \frac{1}{2\pi}\sum_{i=1}^{3}\frac{a_i b_i}{\sqrt{r^2+b_i^2}^3}, \qquad (1)$$

where $a_1 = 0.80$, $a_2 = 0.30$, $a_3 = -0.10$, $(a_1 + a_2 + a_3 = 1)$,
$b_1 = 8.0$ mm, $b_2 = 2.0$ mm, $b_3 = 76$ mm.

The integration of (1) yields the following approximation of the two-dimensional cumulative function

$$F(x,y) = \frac{1}{2\pi}\sum_{i=1}^{3} a_i\left(arctg\left(\frac{x}{b_i}\right) + arctg\left(\frac{y}{b_i}\right) + arctg\left(\frac{xy}{b_i\sqrt{b_i^2+x^2+y^2}}\right)\right) + \frac{1}{4}. \qquad (2)$$

The energy deposited in the square cell of the transverse dimension d is calculated from the values of function (2) in the cell corners:

$$G(x,y) = F(x+\frac{d}{2},y+\frac{d}{2}) - F(x+\frac{d}{2},y-\frac{d}{2}) - F(x-\frac{d}{2},y+\frac{d}{2}) + F(x-\frac{d}{2},y-\frac{d}{2}). \qquad (3)$$

Fig. 1 presents the average value of the energy deposited in a GAMS cell (d=38.4 mm) versus the distance x from the shower axis to the center of this cell for y=0.

The energy calculations with formulas (2) and (3) are bulky and to speed up the calculations it is better to use a more simple approximation. The function shown in fig. 1 is not convenient for such approximation due to a flat part at

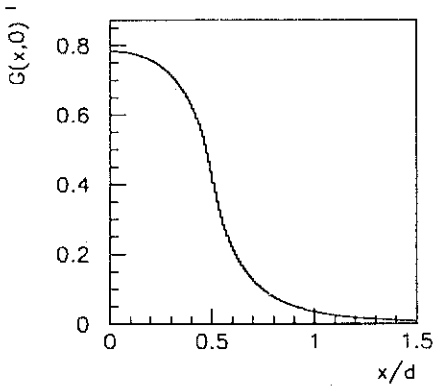


Figure 1. The energy deposited in a GAMS cell as a function of electron coordinate X (Y=0).

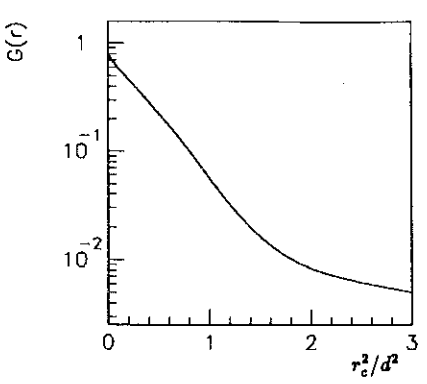


Figure 2. The energy deposited in a GAMS cell (integrated over the azimuth angle $\phi$) as a function of $r_c^2/d^2 = (X_c^2+Y_c^2)/d^2$, where $X_c, Y_c$ are coordinates of the center-of-gravity of electron shower, d is the cell width.

the cell center and a steep slope at the cell boundary. The function looks quite different when the coordinates of the center-of-gravity, $X_c$ and $Y_c$, are used as its arguments. Fig. 2 presents the energy deposited in a GAMS cell as a function of $r_c^2 = X_c^2 + Y_c^2$ integrated over the azimuth angle $\phi = arctg(X_c/Y_c)$.

For approximation, the total range of $G(r_c^2, \phi)$ is split into 5 zones. Inside each zone the function is approximated with the expression $a + b/(r_c^2 + c)$. The $\phi$ dependence is weak, the maximum deviation is less than 0.03, after the corrections made with a table of $10 \times 10$ elements and linear interpolation this value reduces to 0.002. The approximation increases the calculation speed of energy deposited in a cell by an order of magnitude.

## 2. Gamma reconstruction

The gamma reconstruction program uses the shower profile measured for 10 GeV electrons. No difference between the showers produced by electrons or gammas and no energy dependence of the shower profile are assumed. The only correction is a coefficient increasing the shower fluctuations in accordance with the deterioration of the energy resolution of the spectrometer running in a high intensity beam.

The center-of-gravity coordinates $X_c$, $Y_c$ in units of the cell dimension d are used as initial gamma coordinates in the reconstruction program. They are converted to real gamma coordinates only at the last step of gamma reconstruction using the formula

$$X = (X_c + a_1 t)(t^4 + a_2 t^2 + a_3)(t^2 - 1/4)(t^2 - a_4)\, d, \qquad (4)$$

where $t = X_c - X_0$ ($X_0$ is the coordinate of the cell edge nearest to $X_c$, $-0.5 < t < 0.5$) [1], $a_1 = -147$, $a_2 = 0.115$, $a_3 = 0.048$, $a_4 = -0.385$.

The gamma reconstruction program [3] follows three stages.

1. Cluster search. A cluster is one or several neighbouring cells separated from other clusters with zero energy cells. The clusters are analyzed independently.
2. Each cluster may contain several peaks. A peak is located in a cell whose deposited energy is higher than that of any adjoined cell. The program can not find more than 10 peaks in a cluster but in practice such kind of event has never been seen. Peak regions are calculated by sharing the energy deposited in each cell according to the energies expected from the gammas located in each peak region. This is an iterative procedure: after calculating gamma energy and coordinates in each peak the cell energy the sharing is repeated, the number of gammas in the cluster and their energies and coordinates being recalculated.
3. Gamma reconstruction within the peak region. No more than two gammas within a peak region are the main limitation to the program facility. This part of program is completely changed to decrease the number of false gamma produced by inaccurate separation of nearby showers; it is described below.

## 3. Separation of two nearby showers

At the first step only single gamma is assumed to exist in the peak region. The energy integrated over the peak region is taken as its energy. Initial values of the coordinates are calculated from the first moments of X,Y-distribution. A simple fit in two-dimensional space (X and Y) is used to find the minimum of

$$\chi^2 = \sum_{i=1}^{n} \frac{(A_i - E_i)^2}{c^2 A_i (1 - \frac{A_i}{E_0}) + q}\ , \qquad (5)$$

where $A_i$ and $E_i$ are measured and calculated cell energies, $E_0$ is the total gamma energy ($\Sigma_{i=1}^{n} A_i$), c is the constant describing the shower fluctuations (in our case $c^2$=30 MeV), q is a constant which describes the electronics noise (pedestal fluctuations). Since the gamma energy is calculated without fit as the

sum over all cell energies, so the term $1 - \frac{A_i}{E_0}$ is included. If $\chi^2/ND < 3$ (ND is the degree of freedom) the procedure is finished, otherwise the two-gamma hypothesis is taken.

The two gamma separation is done by minimizing (5) with the maximum slope method in three-dimensional space: $\alpha = (E_1 - E_2)/E_0$ , $\Delta X = X_1 - X_2$ and $\Delta Y = Y_1 - Y_2$. The energy and the center-of-gravity coordinates of each gamma are calculated from these variables as well as from total energy $E_0$ and the center-of-gravity coordinates $X_0$ and $Y_0$ of the peak region:

$$E_1 = E_0(1+\alpha)/2, \;\; X_1 = X_0 + \Delta X(1-\alpha)/2, \;\; Y_1 = Y_0 + \Delta Y(1-\alpha)/2,$$
$$E_2 = E_0(1-\alpha)/2, \;\; X_2 = X_0 - \Delta X(1+\alpha)/2, \;\; Y_2 = Y_0 - \Delta Y(1+\alpha)/2. \quad (6)$$

To choose the starting point for the fit, the second central moments are calculated: $M_{xx} = \Sigma_i A_i(X_i - X_0)^2$, $M_{yy} = \Sigma_i A_i(Y_i - Y_0)^2$ and $M_{xy} = \Sigma_i A_i(X_i - X_0)(Y_i - Y_0)$. The axis U with the maximum of the shower width is found from these moments. To estimate the shower asymmetry an additional moment is calculated along this axis: $M_{uu} = \Sigma_i A_i(U_i - U_0)|U_i - U_0|$. The starting values of $\alpha$, $\Delta X$ and $\Delta Y$ are calculated from these moments assuming a thin detector structure (the second central moments do not depend on the shower coordinates). The two-gamma hypothesis is taken if $\chi^2$ becomes smaller than $\chi^2$ in one gamma case by a value, larger than some parameter (it is equal to 5 in this version of the reconstruction program).

## 4. Gamma separation efficiency

To estimate the efficiency of two nearby gamma separation, the isotropic decay $M \rightarrow 2\gamma$ with the energy $E_0$ is generated. Mean values of the cell energies are calculated with (3) and noncorrelated fluctuations are added. The fluctuations correspond to the energy resolution of the spectrometer ($\sigma(E) = c\sqrt{E}$, where $c = 0.15 GeV^{1/2}$). Then the generated events pass the gamma reconstruction program and the efficiency $\epsilon$ of two nearby gamma separation is calculated. The efficiency depends on the energy of each gamma and on the distance between them, so in general case $\epsilon$ is a three-dimensional function.

Fig. 3a shows $\epsilon$, for fixed $E_0 = 10 GeV$, as a function of the distance between gammas and decay asymmetry $\alpha$. One may see (fig. 3b) that if instead of the distance between gammas one uses the value

$$D = \frac{2MZ}{E_0} \quad (7)$$



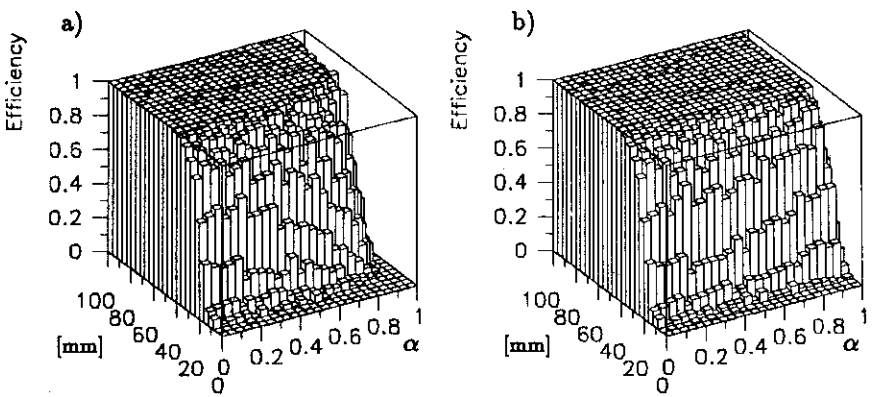


**Figure 3.** **a) The efficiency of two gamma separation as a function of the decay asymmetry $\alpha = (E_1 - E_2)/E_0$ and the distance between gammas.**
**b) The efficiency of two gamma separation as a function of the decay asymmetry $\alpha$ and D (7).**

(Z is the distance from the decay point to the spectrometer), the dependence of $\epsilon$ on $\alpha$ becomes weak, so $\epsilon$ might be presented as a function of two variables ($E_0$ and D). In the case of symmetric decay D is equal to the distance between two gammas.

Fig. 4 presents the efficiency of separation of two nearby gammas with $E_0$=10 GeV as a function of D, dashed line corresponds to the conditions when the program has found only one gamma, the probability to find the third (false) gamma is shown in fig. 5. The 50% level of the separation efficiency corresponds to D=1.9 cm and the probability to find a false gamma does not exceed 0.5%.

A more complicated picture arises during the reconstruction of three nearby gammas (fig. 6, 7). The same value $D = 2MZ/E_0$ is used for the axis X but now M is the effective mass of three gammas. The 50% level of the reconstruction efficiency corresponds to D=7.2 cm. It is determined by the program limitation. (Not more than two gammas in one peak). The probability to find a false gamma achieves 6% (fig. 7). The presence of a peak in this figure is explained by changing the program algorithm when it turns from the searching for two gammas in one peak to the separation of two nearby peaks.

Fig. 8 presents the distribution of $D_{min}$ (minimum of D through each combination of two gammas) for the cases when one gamma out of two is a false one. One can see that as a rule the distance between gammas for such cases is less than 1 cm. In three nearby gamma reconstuction the distance between artificially split gammas is approximately two times larger (fig. 9).

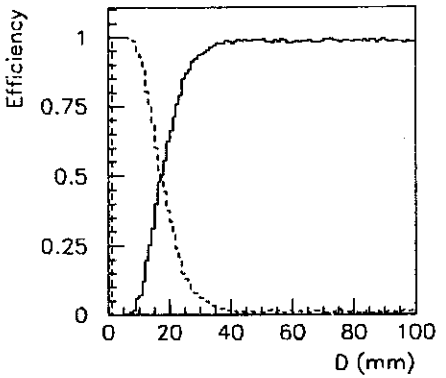


Figure 4. The efficiency of two nearby gamma separation. Dashed line shows the probability to find only one gamma.

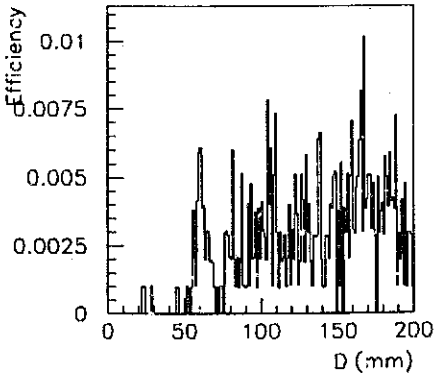


Figure 5. The probability to find a false gamma in the two-gamma separation procedure.

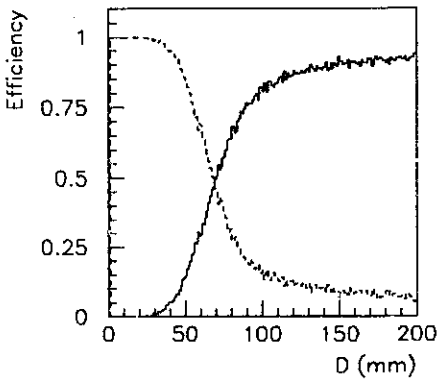


Figure 6. The efficiency of three nearby gamma separation as a function of D (7) calculated for the case of $M \to 3\gamma$ decay. The dashed line shows the probability to find less than three gammas.

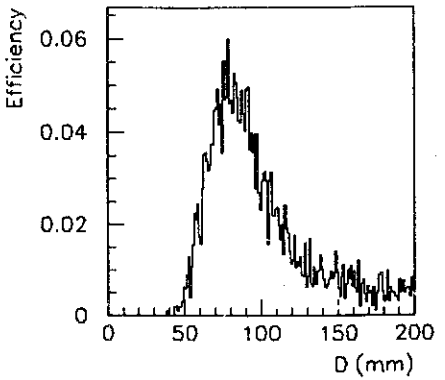


Figure 7. The probability to find a false gamma in the separation of three nearby gammas.



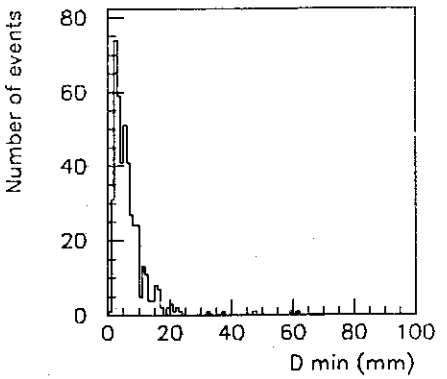


Figure 8. The value $D_{min}$, calculated for the cases when the program finds a false gamma in two-gamma separation.

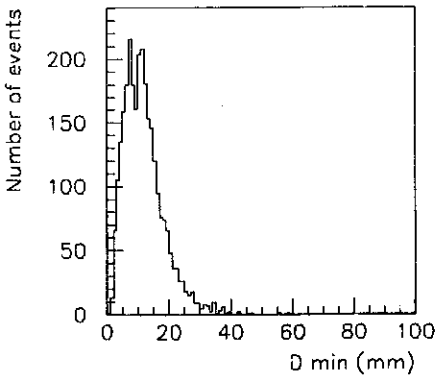


Figure 9. The same as in fig. 8, but for the case of three-gamma separation.

Introducing a threshold for the value $D_{min}$ to the reconstruction program one can reduce the probability to generate a false gamma. The program characteristics with $D_{min} \geq 2cm$ are shown in fig. 10-13. The false gamma in two gamma reconstruction appears with probability 0.1%, the probability to find four gammas in three gamma events does not exceed 0.5%.

The gamma separation efficiency mentioned above is estimated for total gamma energy of $E_0$=10 GeV. The energy dependence of the efficiency is determined by fluctuations of energies deposited in GAMS cells and by the value of the threshold in low energy gamma registration. The efficiencies of two nearby gamma separation for the total gamma energies of 4, 10 and 40 GeV are shown in fig. 14. In separation of three gammas the influence of energy fluctuations is weaker since the separation determines by presence of two peaks in the cluster. The difference in the efficiencies for 10 and 4 GeV (fig. 15) is fully determined by the threshold.

Figures 16 and 17 present the efficiencies of separating two and three nearby gammas calculated for detectors with different cell dimensions. In the range from 20 to 75 mm the 50% efficiency level of separation two gammas follows the linear dependence 0.37d+6 mm, where d is the cell dimension. For the case of three gammas the linear function 1.6d+10 mm also describes the 50% level of the separation efficiency.

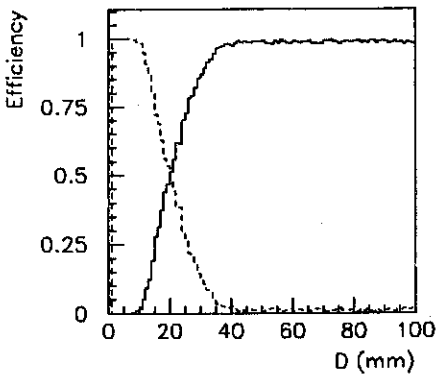


**Figure 10.** The efficiency of two nearby gamma separation for $D_{min} \geq 20$ mm. Dashed line shows the probability to find only one gamma.

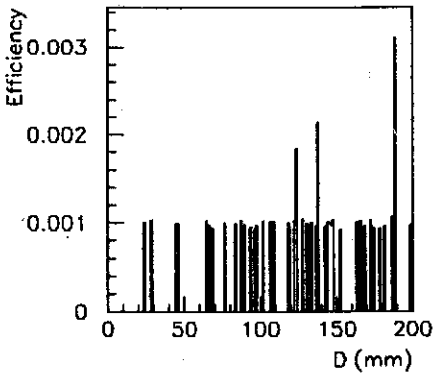


**Figure 11.** The probability to find a false gamma with $D_{min} \geq 20$ mm in the two-gamma separation procedure.

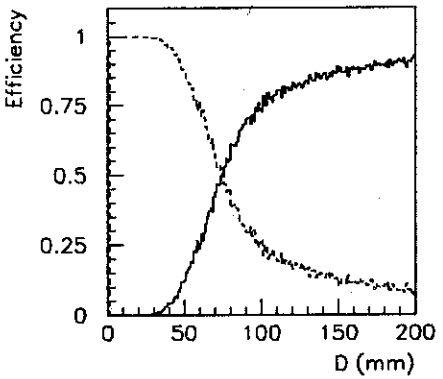


**Figure 12.** The efficiency of three nearby gamma separation as a function of D (7) calculated for the case of $M \rightarrow 3\gamma$ decay, $D_{min} \geq 20$ mm. The dashed line shows the probability to find less than three gammas.

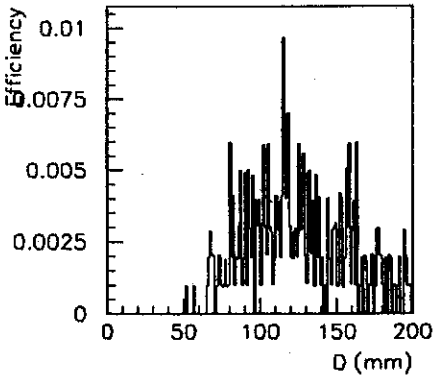


**Figure 13.** The same as in fig. 11, but for the case of three-gamma separation.



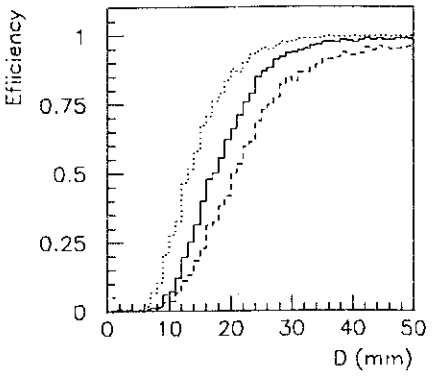


Figure 14. The efficiencies of two nearby gamma separation for the total gamma energies of 4 GeV, 10 GeV and 40 GeV (dashed, solid and dotted lines correspondingly).

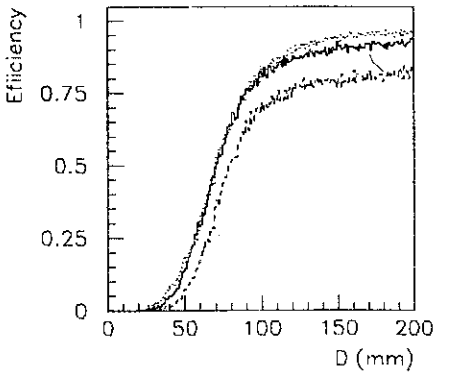


Figure 15. The same as in fig. 14, but for the case of three-gamma separation.

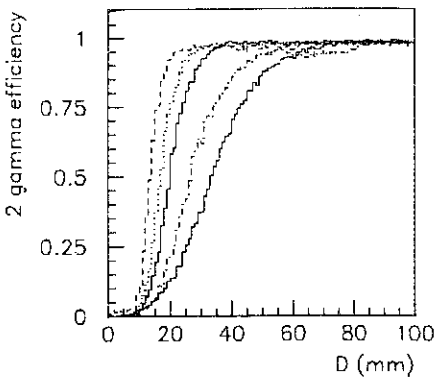


Figure 16. The efficiencies of two nearby gamma separation for the cell dimensions (d) of 20, 30, 38, 50 and 75 mm.

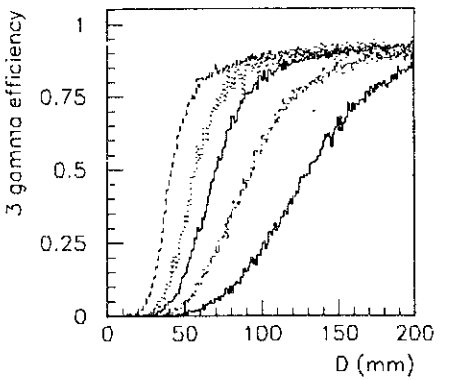


Figure 17. The same as in fig. 16, but for the case of three-gamma separation.

## References

[1] A.A.Lednev, Preprint IHEP 93-152, Protvino, 1993.

[2] F.Binon et al., Nucl. Instr. and Meth. 248 (1986) 86.

[3] A.V.Kulik et al., Preprint IHEP 85-17, Serpukhov, 1985 (in Russian).

*Received December 15, 1993*

А.А.Леднев
Разделение перекрывающихся электромагнитных ливней в ячеистых калориметрах типа ГАМС.

Оригинал-макет подготовлен с помощью системы LaTeX.
Редактор А.А.Антипова

Подписано к печати 28.01.1994 г. Формат 60 × 90/16.
Офсетная печать. Печ.л. 0,60. Уч.-изд.л. 0,74. Тираж 260. Заказ 952.
Индекс 3649. Цена 110 руб. ЛР №020498 06.04.1992.

Институт физики высоких энергий, 142284, Протвино Московской обл.

110 руб. Индекс 3649

ПРЕПРИНТ 93-153, ИФВЭ, 1993